Temperature dependence of liquid lithium film formation and deuterium retention on hot W samples studied by LID-QMS. Im....

Article *in* Nuclear Fusion · January 2018

DOI: 10.1088/1741-4326/aaa8d0

CITATION
1

READS
18

4 authors, including:

Alfonso De Castro
Centro Investigaciones Energéticas, Medioa…
19 PUBLICATIONS **29** CITATIONS
SEE PROFILE

Francisco L Tabares
Centro Investigaciones Energéticas, Medioa…
302 PUBLICATIONS **2,188** CITATIONS
SEE PROFILE

Temperature dependence of liquid lithium film formation and deuterium retention on hot W samples studied by LID-QMS. Implications for future fusion reactors

To cite this article before publication: Alfonso de Castro *et al* 2018 *Nucl. Fusion* in press https://doi.org/10.1088/1741-4326/aaa8d0

Temperature dependence of liquid lithium film formation and deuterium retention on hot W samples studied by LID-QMS. Implications for future fusion reactors

A. de Castro [a,*], A. Sepetys[b], M. González[a] and F.L. Tabarés [a]

[a]*Fusion National Laboratory-CIEMAT, Av. Complutense 40, 28040 Madrid, Spain*

[b]*CEA, IRFM, 13018 St. Paul-lez-Durance, France*

Abstract

Liquid metal (LM) divertor concepts explore an alternative solution to the challenging power/particle exhaust issues in future magnetic fusion reactors. Among them, lithium (Li) is the most promising material. Its use has shown important advantages in terms of improved H-mode plasma confinement and heat handling capabilities. In such scenario, a possible combination of tungsten (W) on the first wall and liquid Li on the divertor could be an acceptable solution, but several issues related to material compatibility remain open. In particular, the co-deposition of Li and hydrogen isotopes on W components could increase the associated tritium retention and represent a safety risk, especially if these co-deposits can uncontrollably grow in remote/plasma shadowed zones of the first wall. In this work, the retention of Li and deuterium (D) on tungsten at different surface temperature (200ºC-400ºC) has been studied by exposing W samples to Li evaporation under several D_2 gaseous environments. Deuterium retention in the W-Li films has been quantified by using Laser Induced Desorption-Mass Spectrometry (LID-QMS). Additional techniques as Thermal Desorption Spectroscopy, Secondary Ion Mass Spectrometry, profilemetry and Flame Atomic Emission Spectroscopy were implemented to corroborate the retention results and for the qualitative and quantitative characterization of the films. The results showed a negligible (below LID sensibility) D uptake at $T_{surface}$=225ºC, when the W-Li layer is exposed to simultaneous Li evaporation and D_2 gas exposition (0.67 Pa). Pre-lithiated samples were also exposed to higher D_2 pressures (133.3 Pa) at different temperatures (200ºC-400ºC). A non-linear drastic reduction in the D retention with increasing temperatures was found on the W-Li films, presenting a D/Li atomic ratio at 400ºC lower than 0.1 at.% on a thin film of ≈ 100 nm thick. These results bode well (in terms of tritium inventory) for the potential utilization of this material combination in a real reactor scenario.

*Corresponding author address: **Av. Complutense 40, 28040 Madrid, Spain**

*Corresponding author E-mail: **alfonso.decastro@ciemat.es**

Keywords: **Co-deposition, Deuterium retention, Tungsten, Lithium, LID, Fusion reactors**

1. Introduction

The research in the field of Plasma Facing Materials (PFMs) is decisive for the development of magnetic nuclear fusion energy and the economic viability of commercial reactors. At present, after decades of intense investigation, tungsten (W) has become the main candidate to be used in future reactors and it has been selected to be used in the ITER divertor [1-2]. Among the main problems related with the surrounding materials exposed to burning D-T plasma during the operation of a future reactor, the hydrogen isotope retention (tritium inventory) and the power exhaust handling are among the most challenging issues to be solved for the successful development of fusion energy. In ITER during short pulsed operation, the acceptable nominal power load in the divertor region must be limited to 10 MW/m^2 while transient events as Edge Localized Modes (ELMs), disruptions, runaways and other uncontrolled events can increase the heat loads up to 1 GW/m^2 [3]. Moreover, it is evident that the longer pulsed mode operation and the associated neutron fluxes will affect to the power handling and associated PFM damage in a reactor prototype as DEMO, thus making the removal of power exhaust and the concomitant PFMs degradation even more demanding.

Liquid metal (LM) components (in particular lithium, Li) offer an innovative solution to this issue as its surface is, in principle, free of irreversible damage. The use of Li in several magnetic devices has shown unique advantages in terms of plasma confinement improvement (at wall temperatures much lower compared to the proposed in the following sections of this paper for a first wall low hydrogenic retention DEMO scenario) and heat handling capabilities [4-6], becoming an option that is currently studied in alternative divertor concepts [7]. Despite these positive effects, the main drawback associated with the use of liquid lithium is probably its strong affinity with hydrogen isotopes as a result of its alkaline and very reactive nature. As the total moveable tritium inventory for the in vessel components is limited to 700 g [8], the potential tritium uptake of Li PFM could suppose a serious risk for D-T operation.

Considering a DEMO scenario combining a conservative solid (hot) tungsten first wall and a liquid Li element at the divertor, where the power exhaust is concentrated and mitigated, as viable in terms of technology and engineering development, the fuel retention problem on the divertor could be solved by periodic baking at $T \leq 550^{o}C$ [5] or ultimately, with recirculating closed loop solutions [9-11]. These ideas propose the recirculation of liquid lithium present in the PFCs out of the vessel to be re-injected in

the divertor components after its regeneration (with the total desorption of the hydrogen isotopes from Li elements at moderate temperatures [12-14]). Notwithstanding, for the development of these alternative solutions, other issues related with this material compatibility in terms of material migration and mixing (among others) must be investigated. Unavoidably, in a future reactor the continuous plasma bombardment onto the PFM will produce its sputtering. With this W-Li PFM considered scenario, the creation of mixed W-Li films, with deposition of W on Li and vice versa will take place. Moreover, the effects of the associated neutron flux (that is expected to create defects and traps in the materials, increasing in this way the associated fuel retention) in these processes needs to be taken into account for the global integration of this PFM solution in a reactor. All these issues, however, are out of the scope of this paper.

Concerning tritium inventory build-up, the presence of liquid lithium on the divertor will produce evaporative Li fluxes and a concomitant thermal co-deposition of Li atoms on W surfaces that will be associated with an increase in the fuel retention on such films. In the last years, intense experimental and modelling work has addressed the surface temperature influence on the behaviour/stability of Li-D containing films deposited in different substrates as well as several issues that would be associated with the possible integration of this PFM solution in a reactor environment. Thus for example, the results of a surface analysis study on nickel [17] substrates, on which LiH films were created, indicated unstable hydride (LiH) films when the surface temperature was increased up to 340ºC. This behaviour was found in ultrathin (0.5-10 monolayer, thickness <3 nm) LiH films. Additionally, Capece et al. [18] also studied the temperature effect on the D retention in ultrathin lithium films deposited on molybdenum (TZM) alloy confirming the decomposition of lithium deuteride at temperatures below 400ºC. Another important related aspect is the material erosion by sputtering of liquid Li-D containing films. This issue was firstly studied by Allain et al. [19] being also investigated in the NSTX device [20] on liquid lithium deposited on graphite and molybdenum substrates. They found increasing sputtering yields for higher temperatures in Li-D and Li-Li self-sputtering [21]. In NSTX [20] an enhancement (factor 2) in the Li sputtering was found at temperatures between 400ºC-500ºC compared to 200ºC. Moreover, preferential sputtering of the D atoms present in Li-D containing films was found [22]. These results would imply a reduction of the Li film thickness deposited on W and especially in the fuel retention in such films during the

reactor operation, but it would lead to an increase in the input flux of Li impurities to the burning plasma. However, for the global evaluation of the plasma contamination by Li impurity at $T_{Lithium}$>400ºC, evaporative fluxes rather than sputtering will dominate [16, 23]. Due to the exponential increase of the vapour pressure with temperature and the associated increase in the plasma contamination, conservative estimates have establish the upper limit for the temperature of the liquid lithium surfaces to values around 450ºC [23] in order to maintain a suitable plasma core confinement, thus avoiding its excessive dilution by Li impurities and the associated quenching of the D-T reactions. However, the utilization of temperature limits higher than 450ºC for the liquid Li surfaces could be possible as different works [24-26] have shown that even a lithium ion concentration higher than 10% in the plasma core (concentration that would be associated to $T_{surface}^{Li}$>450ºC [26]) would be still compatible with the necessary confinement for the maintenance of the D-T burning plasma conditions.

The scope of this paper is the study of the thermal deposition of lithium and molecular D_2 on tungsten, trying to analyze the potential problem derived from an uncontrolled growth of thick Li co-deposits in remote parts and/or plasma shadowed zones of the W first wall. On these parts this issue could be especially problematic due to the impossibility of direct cleaning by the plasma itself and/or auxiliary discharges without the replacement of the involved elements. Laser Induced Desorption (LID) assisted by mass spectrometry (QMS) was used to remove and quantify the deuterium uptake on W-Li-D containing films after the deposition of Li and deuterium (D) on tungsten, emphasizing on the dependency of the surface temperature on the net deuterium retention in such films.

The paper is structured as follows. Section 2 introduces the experimental setups and the work devoted to produce the W-Li-D samples, their laser irradiation and post mortem analyses. The experimental results (LID, TDS, SIMS, profilemetry and FAES) are described in section 3. Section 4 discusses the experimental findings, relating them with the thermodynamic aspects of the thermal dependence of the deuterium absorption on the W-Li films as well as the possible implications of the obtained results in the potential application of the proposed PFM solution in a reactor scenario. Finally, section 5 summarizes the main conclusions obtained from this extensive experimental work.

2. Installations, procedures and techniques utilized during the experimentation

The experimental works performed during these studies can be divided into three separated phases:

- 1) Preparation of the W-Li-D samples by means of its deposition under different Li-D_2 environments.
- 2) LID measurements after transportation of the samples in closed manipulators over-pressurized with dry argon to avoid atmospheric contamination.
- 3) Application of post mortem techniques for the total characterization of the W-Li-D films.

2.1. Preparation of W-Li-D samples

The deposition of lithium and deuterium on tungsten (cold rolled and high purity) rectangular (20.4 mm length, 17.5 mm width and 0.1 mm thick with an exposed area of 3.6 cm^2 and total mass, m=0.72±0.04 g) samples was carried out in a stainless steel vacuum vessel (deposition chamber illustrated in Figure 1) with an approximated volume of 5 L, pumped out by means of a turbomolecular pump in serial connection with a rough pump. Two different kind of Li-D_2 interaction environments were used to prepare the samples:

- Simultaneous exposure to evaporative Li and gaseous D_2 (co-deposition regime) under a D_2 atmosphere ($p^{D_2}_{chamber}$ = 0.67 Pa).
- Sequential exposure to Li and gaseous D_2. Firstly, lithium was pre-deposited on W before exposing the created film to D_2 at a higher pressure conditions (≈133 Pa). Three different samples were prepared by changing the surface temperature (200ºC, 300ºC and 400ºC) during the Li and D_2 exposure.

2.1.1. Simultaneous deposition of deuterium and lithium on W.

One sample (named as wlid) was prepared by evaporating lithium in a molecular D_2 (0.67 Pa) environment while the sample temperature was maintained around 200-225ºC. This procedure, which could be denominated as thermal co-deposition, tried to simulate the molecular pressure levels existent on remote or plasma shadowed areas of a fusion reactor first wall during D-T operation.

Inside the deposition chamber a stainless steel oven (2.5 cm of diameter and 4 cm of height) filled with 2 grams of lithium was placed. The Li atoms were effused through a circular hole (d=1 cm) situated on the top of the oven. This device acted as a Knudsen

cell for the Li atoms during the sample preparation procedure. The oven was heated up by using an electric resistance rolled around it. The lithium temperature during the process was measured with a type K thermocouple inserted in the Li bulk. A good equivalence between the measured temperature and the Li one was registered as the melting of the Li was visualized, with its corresponding temperature plateau, at 178ºC in the thermocouple, while $T_{melting}^{Li}$ is 180.5ºC).

The tungsten samples were washed out in an ultrasound bath followed by baking (150ºC) and finally cleaned with acetone and ethanol to eliminate dust and impurities. After this sample conditioning protocol, that is common for all the samples considered in this study, they were placed in a 30 cm length manipulator installed in the deposition chamber coupled with a gate valve. The sample was positioned at a distance of 26.5 mm, perpendicularly oriented to the oven effusion hole (see Figure 2), forming its edges angles of φ_1= 12º and φ_2=35º respect the normal direction to the effusion source. In this way, the sample encompasses an approximate solid angle (ω) of around 0.63 sr respect the evaporation semispherical surface of the oven hole. As a consequence of the proximity of the sample during the oven heating for the Li evaporation, the radiation increases the sample temperature up to 200-225ºC. The temperature on the tungsten surface was measured using an infrared pyrometer (150-1000ºC measurement range). An ionization gauge (Bayard Alpert) was used to monitor de vacuum level inside the vessel (residual pressure around 10^{-5} Pa). Before starting the co-deposition, the sample was heated up to 550ºC during 30 minutes to degas residual water and hydrogen. The heating was performed with a W resistive filament, fed with a DC power supply, placed by means of other manipulator behind the sample holder very close but detached from it. The lithium bulk and oven were also outgassed (up to 300-325ºC) during 30 minutes. This general description and outgassing procedures were applied in the preparation of all the samples considered in this study.

After this procedure, the lithium present inside the oven is heated up to 450ºC. When it reaches this value, the deuterium gas is introduced in the chamber through a leak valve up to a total pressure of 0.67 Pa (capacitance manometer measurement) during 30 minutes in a continuous flow regime. The temperature of the sample was monitored with the pyrometer, oscillating between 200-225ºC during all the exposure. A simple calculation of the evaporative flux of Li atoms gives a total number of evaporated lithium atoms in the oven around $4.3 \cdot 10^{20}$ during the whole oven heating procedure.

Taking into account the angular position of the sample and the solid angle the total number of reaching Li atoms to the sample is estimated around $1.5 \cdot 10^{19}$ that roughly implies an average lithium film thickness of ~1 µm.

After this Li-D_2 exposure, the sample is prepared for the LID analysis. The manipulator is retracted, the whole chamber is vented with Argon and the manipulator gate valve is closed in over-pressure conditions. Then, the manipulator is transported from the deposition chamber to the LID chamber avoiding in this way, an atmospheric sample contamination that can affect to the Li-D films [27-29].

2.1.2. Pre-deposition of lithium on tungsten followed by high pressure D_2 gas exposition.

In this case, pre-lithiation of the tungsten samples was performed by evaporating Li at 450ºC from the oven during 30 minutes in vacuum conditions (surface temperature around 200-225ºC on sample). After the pre-lithiation, the sample is exposed to a higher D_2 pressure environment (133 Pa) for 1 hour. At the beginning of the D_2 exposure, the gate valve that connects the turbopump with the deposition chamber is closed to maintain this deuterium pressure without external puffing in static conditions (no pumping). It is important to note that the deuterium exposition must be started when the temperature of the lithium present in the oven is below its melting point to avoid its exposure to deuterium in liquid state. Previous trials showed that if deuterium is injected in the deposition chamber immediately after the deposition of lithium on the sample when it is still hot and liquid inside the oven, the liquid surface and bulk, that contains several grams, act as a sink for the D_2 molecules, avoiding the interaction of deuterium with the W-Li layer of the sample. In our experiments the exposure of the pre-lithiated samples to deuterium was carried out with temperatures lower than 100ºC inside the oven in all instances. However for the case of the simultaneous exposition with D_2 and Li (sample named as wlid, whose preparation was explained in the previous section), the exposure regime was a continuous gas injection, determining a D_2 pressure in the chamber of 0.67 Pa, with continuous pumping. With this regime, it was possible to maintain the D_2 pressure level (0.67 Pa) with a lithium temperature of 450ºC in the oven, thus allowing the simultaneous exposure to Li and D_2 on the W sample.

This necessary cooling time of around 90 minutes for the pre-lithiated samples would unavoidably imply a contamination (oxidation) due to the interaction with residual

gaseous molecules associated to the vacuum levels. Such levels (~10^{-5} Pa) can involve, considering that the total residual vacuum is exclusively water as extremely worst case approximation, an oxygenic impurity growth rate (as we do not have a proper in situ analysis, we generally consider them as LiO_x) on the sample surface of ~0.5 monolayers (ML) per minute [30]. Hence, the cooling time would produce a total amount of 10^{17} impurity particles present on sample surface (assuming 1 ML≈$6\cdot10^{14}$ particles/cm^2 [31]) and A_{sample}=3.6 cm^2). Even in this extreme case, the impurity amount would be small compared to the remaining Li after the exposure to D_2 on samples as the FAES analyses gave a minimum lithium content on samples around 10^{18} atoms, for the case of the sample wlid8 (see table 5). This experimental contamination of the Li films can produce a higher retention as has been experimentally and theoretically demonstrated in lithium-conditioned carbon walls [32]. However, our pre-lithiated samples did not contain any carbon content and the expected impurity deposition prior the D_2 exposure resulted much lower. As will be shown in section 3.2.2, the SIMS analyses showed a very low content of such lithium impurities compared to the pure lithium content. Hence, in principle, the major part of this retention can be considered due to the pure lithium films. Consequently, the unavoidable lithium impurity presence on samples may play a certain role in the retention, probably increasing it, but their effect in the global results can be considered small. Three different surface temperatures during the D_2 exposure were studied: 200ºC (sample named as wlid6), 300ºC (wlid8) and 400ºC (wlid10), assuring in this way that pre-deposited lithium is in the liquid state in all instances. The heating of the pre-lithiated samples during the starting of the exposure to deuterium produced the partial melting of the pre-deposited lithium on the vertical surface of the sample. In these conditions the gravity force acts on the liquid vertical surface producing partial lithium losses due to its dripping from the sample. After the complete preparation of the pre-lithiated samples, the same procedure to transfer the samples to the LID chamber was carried out. Additionally, for the case with highest lithium and deuterium content, (pre-lithiation + D_2 exposure at 200ºC), another two samples (named as wlid11 and wlid13) were prepared and their D content was measured by LID in order to check the reproducibility of the technique and the consistency of the results.

2.1.3. Preparation of a tungsten blank sample

Finally a blank tungsten sample (wlid12) was prepared in order to compare the deuterium retention values of the W-Li films with the uptake of the lithium-free

tungsten surface. After its outgassing, it was exposed to a D_2 gaseous environment (p=133 Pa during 1 hour).

2.2. Irradiation of W-Li-D samples with the Nd:YAG laser beam

Among laser methods [33], LID enables the *in situ* fuel removal and the measurement of the retained hydrogen isotopes under high vacuum conditions. In our case the desorbed hydrogen is detected and measured with a SRS 100 residual gas analyzer (RGA). For the irradiation of the samples a solid state (Nd:YAG) laser (LITRON LPY 600) operating in the first harmonic (1064 nm) and long pulse mode (τ = 0.25 ms) has been used [34]. The average output of energy per pulse was 1067 ± 47 mJ. Measurements of beam energy were carried out by means of a pyroelectric joule meter. The original spot size of the laser was measured (sensibility of 0.2 mm), presenting an approximate Gaussian distribution (close to top hat profile) with a full width half maximum value (FWHM) of 6.5 mm, corresponding to energy and power density values of 3.3 Jcm^{-2} and 13 $kWcm^{-2}$. After focusing the laser with a converging lens (f=400 mm), a beam diameter of 1.25 mm is obtained (see section 3.3.3.). Consequently, the energetic characteristic of the laser were increased up to 90 Jcm^{-2} and 360 $kWcm^{-2}$. In all the analyses a frequency of 1 Hz was used. In order to estimate roughly the absorbed laser power, the energy losses due to reflection in the W-Li surfaces need to be taken into account. The reflectance (R) of W and Li exposed to infrared light (1064 nm) can be found in [35], being 0.60 the global value for tungsten and 0.94 for solid lithium. As will be explained later in the profilemetry sections, the non-homogeneity of the deposition process produced an irregular surface, as the profilemetry measurements demonstrated, showing zones with Li shortage with almost unique presence of W on surface. This deposition morphology existed before applying the laser shots. Moreover, the lithium film thickness constituted only a few microns that compared to the total thickness of the W substrate (100 μm) represents a very small fraction. Additionally, lithium melting was produced during the laser pulse and for liquid lithium the reflectance decreases, giving values of 0.7 at $T_{melting}^{Li}$ and 0.6 at $2 \cdot T_{melting}^{Li}$ [36]). In such situation, the propagation of the pulsed heat flux is expected to be more pronounced. Consequently, taking into account all these particularities, for analysing the global thermal transfer in the z direction, to use an average value, between W and Li, for the reflectance, as well as for the thermo-physical values as diffusivity, etc, seems much more reasonable than use the normal values for solid lithium. The rest of the thermal

characteristics for tungsten [37], lithium [38] and mean values between both elements, are presented together with the reflectance values in Table 1.

The amount of hydrogen isotope desorbed from the hot spot will depend on the maximum temperature achieved on the surface during laser irradiation. This pulsed temperature change can be modeled by following the Fourier's law of heat conduction. Assuming several simplifications [39], the solution of the one dimensional differential heat equation [40] gives the evolution of the temperature (T) at a depth z and time lower or equal to the laser pulse length (τ):

$$T(z,t \le \tau) = T_0 + \frac{2I_0(1-R)}{k} \cdot \sqrt{Dt} \cdot ierfc\left(\frac{z}{2\sqrt{Dt}}\right). \quad (1)$$

In this expression, ierfc is the integral of the complementary error function that can be evaluated in terms of the error function, R is the reflectance for the irradiated surface, k is the thermal conductivity and D represents the thermal diffusivity. For a time greater than the pulse duration the temperature profile can be evaluated introducing another term delayed in a time factor (t-τ) [40]. Applying this equation, computer simulations were performed in order to evaluate the temperature changes induced on the samples.

The simulations showed maximum temperatures between 900ºC-600ºC depending on the z position. Even for the deepest point (100 µm) situated at the farthest distance from the laser beam incidence, the temperature rose up to 600ºC. Several experimental results have shown that the hydrogenic desorption from lithium is completed at these temperatures [12-14]. Consequently, these calculations indicated that the laser shot would be able to heat the sample and induce the total hydrogenic desorption. In any case, more diagnostics and post mortem analysis were performed to assure the complete removal of the hydrogenic content.

Once the samples are prepared and transported without atmospheric contamination to the LID facility, the manipulator is connected to the LID chamber whose elements are listed in Figure 3. An intermediate small port connects the manipulator valve with the main valve of the LID chamber. This port is assembled to a mobile pumping unit before opening the manipulator valve, avoiding in this way the contact of the sample with air. Before introducing the sample in the LID chamber, it is necessary to pre-pump the manipulator (during 2-3 hours) with the mobile pumping unit to adequate its pressure to the very high vacuum conditions of the LID chamber (≈0.8-1·10^{-5} Pa). After introducing

the sample in the LID chamber, the whole setup is pumped out for ~12 hours to reach the existing previous vacuum level before connecting the manipulator. This procedure allow assuring optimal vacuum levels inside the LID chamber, that are necessary for a good analysis avoiding in this way the increase in the residual contents of deuterium, hydrogen, HD and water inside the chamber. In principle, the interaction of the Li-D containing films with the residual vacuum during this pumping period would be able to produce the formation of impurities as was previously commented in section 2.1.2. Taking into account the same reasoning, the longer exposure time could create in the worst case an impurity layer comparable (same order of magnitude) to the total lithium content of samples. Although no LID analyses were performed in order to search oxygen or water desorption from impurities (Li oxides or hydroxides), the SIMS results showed a very low presence of such impurities compared to lithium (see section 3.2.2 for further details), hence the formation of impurities on the Li layer during the pumping periods can be considered as not very significant.

Different LID analyses were performed on the sample, changing the position of the laser spot and the gaseous species that is measured (D_2, H_2, HD). With the RGA measurements to get enough time resolution (≈70 ms) of the desorption peaks, the device must be operated in the leak test mode. In this mode, only one species can be measured in each laser shot. Consequently it was no possible to measure the content of more than one molecule at the same point of the sample. Therefore, the determination of the different hydrogenic species must be carried out in different points of the samples. Differences on the Li/hydrogenic content depending on the position of the samples are expected as a result of the non-homogeneous deposition of lithium on sample and the concomitant deuterium absorption. Several measurements for each hydrogenic molecule were performed to average the results. In each laser spot the irradiation is repeated several times until the residual peaks obtained by the RGA are smaller than the 5% of the first peak. These peaks are attributed to lateral propagation of the laser radiation that induces hydrogenic desorption from adjacent (lateral) points to the laser spot. At this moment, it is considered that the total desorption on the spot has taken place. Normally it happened after 2-3 laser shots on the sample spot. In the samples with highest lithium content, that made possible its direct easy visualization (e.g. wlid6), the removal of the whole lithium layer on the laser spots was clearly visible after this procedure, thus

indicating the concomitant full removal of deuterium, that posteriorly was corroborated by the morphology of the LID craters (see profilemetry section, numbered as 3.2.3)

By calibrating absolutely the mass to charge ratio, the signals associated to the hydrogenic molecules (2 amu/e for H_2, 3 amu/e for HD and 4 amu/e for D_2) can be quantified. This work (calibrated leak method) relates the single RGA peaks to absolute flux values (molecules/s) allowing the absolute quantification of the desorbed products. The concomitant mass to charge ratio signal, obtained by subtracting previously the background level of the signal with no input flux into the chamber, can be translated to molecular flow. By integrating the peaks registered by the RGA the retained hydrogenic content can be absolutely quantified. This calibration procedure was performed separately for hydrogen (calibration respect to 2 amu/e) and deuterium (respect to 4 amu/e). For the mixed specie, as pure HD gas bottles were not available at laboratory, the absolute calibration cannot be performed. Consequently for HD, an intermediate value between the calibration constants for hydrogen and deuterium was used in the quantification. During the RGA measurements associated to LID a special care was taken to ensure a sampling rate fast enough (~70 ms) to not distort the temporal shape of the desorbed peaks. Figure 4 shows that the RGA obtained signal is quasi-coincident compared with the corresponding pressure signal (Ionization gauge sensor) measured with a faster sampling rate (5 ms) during the desorption induced by the laser shot, thus confirming a proper RGA data sampling.

2.3. Post-mortem analyzes on samples

2.3.1. Thermal Desorption Spectroscopy

In order to compare the retention values obtained by LID with other absolute quantification technique, thermal desorption spectroscopy analyses (TDS) assisted with mass spectrometry (RGA measurements) were implemented on the samples wlid11 and wlid13 after its LID irradiation. Again, the samples transportation was the same previously detailed to avoid atmospheric contamination. Inside the deposition chamber, the samples were heated up by using the tungsten filament described in section 2.1.1. The surface temperature of the sample was measured with the optical pyrometer and desorption was followed registering the changes on the chamber pressure with an ionization gauge. Additionally, a SRS 100 mass spectrometer, identical to the previous one used in the LID measurements, was installed in the deposition chamber trying to

follow the thermal desorption. Unfortunately the increase in the pressure produced the saturation of the RGA filament and the failure in the mensuration. Before starting the TDS measurement, the W filament used for the sample heating was outgassed by feeding it with the maximum power during 30 minutes in order to eliminate water, hydrogenic molecules or another volatile species that could disturb the changes in the pressure measured during the analysis. This outgassing was performed with the sample situated in a completely retracted position along the manipulator to maintain it at room temperature and not produce any desorption from it due to residual heating induced by the filament. In this way, the increase in the pressure can be approximated as produced mostly due to the deuterium desorption that are the majority volatile component of samples, giving the result a maximum limit for the deuterium retention. Finally, a calibration work for the absolute pressure signal respect to deuterium fluxes introduced in the chamber (equivalent to the explained in section 2.2) was performed to absolutely quantify the deuterium retention.

2.3.2. SIMS analyzes

SIMS measurements were carried out on three samples: the wlid6 sample (pre-lithiated and exposed to deuterium at 200ºC), the wlid8 sample (pre-lithiated and exposed to D_2 at 300ºC) and the wlid12 sample (blank). Transportation of the samples from LID to SIMS vacuum chambers was carried out by using the same procedure previously explained for the LID analyzes with the used manipulator over-pressurized with dry argon. To identify the elements and compounds present on the sample surface layer a static SIMS analysis (mass to charge ratio scan, m/q) was performed as the first step of the analytical procedure.

Two different mass scans were performed. The first one from 0 to 80 amu/e, in order to identify hydrogenic species (H_2 at 2 amu/e, HD at 3 amu/e and D_2 at 4 amu/e), Li isotopes (^{6}Li and ^{7}Li), oxygen from the ion beam, residual water molecules (amu/e 18-20) and the presence of Li impurities due to the atmospheric contamination: lithium oxides (amu/e 28-30 and LiO clusters from oxide cracking at amu/e 22-23), lithium hydroxides (amu/e 23-25) and lithium carbonates (amu/e 72-74). The second mass scan covered the amu/e range from 180 to 220 in order to recognize the W isotopes (amu/e 182-186) and the possible associated oxides (amu/e 198-202) and lithium combinations (amu/e 188-193). After the identification of the main elements and compounds, dynamic

SIMS analyses were performed in order to study the depth profiles of the more interesting constituents. Among the several mass to charge signals measured in this dynamic SIMS, four of them were particularly interesting due to the lack of overlapping with other isotopologue species: 4 amu/e that is directly related with D_2, 6 amu/e (^{6}Li), 9 amu/e (^{7}LiD) and 184 amu/e (^{184}W). Both static and dynamic (with simple electrostatic quadrupole detection) SIMS analyses were performed with O_2^+ primary ion beam in a Hiden SIMS Workstation experimental unit. The residual vacuum determined a pressure around $5 \cdot 10^{-5}$ Pa inside the chamber during the measurements, while the characteristics of the primary ion beam were a nominal emission current of 500 nA and beam energy of 5 keV.

2.3.3. Profilemetry measurements

This technique was used to estimate the size (diameter) of the LID craters Furthermore, other measurements were performed in order to estimate the thickness of the lithium layer deposited on tungsten comparing the level of this Li layer to the (lithium free) W surface situated below the sample holder tab used for the sample fastening during its Li-D_2 exposure. In principle, small deviations and/or inclinations in the sample surface can exist. However, the profilemeter software was equipped with a specific tool for the (virtual) alignment of the crater lateral boundaries as well as the alignment of remaining Li surface in the case of the involved Li thickness measurements. This alignment protocol was carried out before starting the profilemetry analysis. In this way, the obtained results cannot be attributed to any sample surface inclination and/or deviation. These profilemetry measurements were carried out in atmospheric conditions without protecting the lithium films from contamination. No chance of performing them on a vacuum environment was possible. For the measurements a 2-D stylus profilemeter (Bruker DektakXT) with a vertical resolution of 1 nm was used. A picture of a LID crater present on the W-Li surface of a sample is represented in Figure 5. Although in the figure the geometrical shape of the crater seems ellipsoidal due to the picture deformation induced by the perspective of the profilemeter camera lens, specific measurements of the diameter in both X and Y axis shown that the craters were approximately circular.

2.3.4. Flame atomic emission spectrometry (FAES) for quantification of the deposited lithium.

After the application of these techniques, aqueous Li dissolutions were prepared by immersing the W-Li samples in 50 mL of hot ultrapure (Milli-Q®) water. Then, they were sent to the chemistry laboratory that carried out the FAES analysis to determine the total lithium content of the samples. This procedure was performed for the wlid (simultaneously exposed to Li-D_2 environment) and the pre-lithiated (wlid6, wlid8, wlid10, wlid11 and wlid13) samples. Furthermore, other samples were prepared for FAES determination in order to compare the formation of the lithium film on the W surfaces depending on the deposition conditions (gas presence or absence, pressure and surface temperature). Two different sets of additional samples were prepared:

- Samples exposed to lithium evaporation in high vacuum conditions ($p \approx 6 \cdot 10^{-5}$ Pa). The evaporation also took place at 450ºC in the lithium oven. Three samples were prepared at different $T_{surface}$: 200ºC, 300ºC and 400ºC. These samples were not later exposed to any D_2 exposure, thus avoiding the concomitant and additional surface heating that eliminates a part of the lithium film due to its melting and dripping. In this way the removal of lithium due these effects can be directly evaluated by comparing the lithium thickness in this group of samples with the obtained for the pre-lithiated samples.
- Samples exposed to lithium deposition under a helium atmosphere at p=0.67 Pa. Evaporation of lithium was carried out under the identical conditions employed for the preparation of the wlid sample but changing the D_2 atmosphere by helium one, in order to compare the influence of the presence of an inert gas instead of D_2 that in principle can interact with the lithium atoms. Different samples were prepared at surface temperatures of 200ºC, 300ºC, 400ºC and 500ºC.

3. Experimental results

3.1. Deuterium and hydrogen retention by LID

The number of hydrogenic molecules desorbed from the irradiated sample spots is calculated by integrating the registered RGA peaks over the time and summing these integrated peaks as these equations show:

$$H_2^{des} = K_{H2} \cdot \sum_{i=1}^{n} \int (2Amu/e - background) \cdot dt \,, \quad (2)$$

$$HD^{des} = K_{HD} \cdot \sum_{i=1}^{n} \int (3Amu/e - background)\,dt \text{ , (3)}$$

$$D_2^{des} = K_{D2} \cdot \sum_{i=1}^{n} \int (4Amu/e - background) \cdot dt \text{ , (4)}$$

being K_{D_2}, K_{H_2} and K_{HD} the values of the calibration constants for D_2, H_2 and HD. With these values, the hydrogenic areal densities are directly obtained with the equations 5 and 6:

$$D_{ret} = \frac{2 \cdot D_2^{des} + HD^{des}}{A_{spot}} \text{ , (5)}$$

$$H_{ret} = \frac{2 \cdot H_2^{des} + HD^{des}}{A_{spot}} \text{ , (6)}$$

The profilemetry measurements (see section 3.2.3.) yielded a mean spot diameter of 0.125 cm. Hence, by considering it as approximately circular, the desorption area is $A_{spot} \approx 0.0123$ cm^2. To obtain the retention values for hydrogen and deuterium (H_{ret} and D_{ret}) several sample points were analysed with the laser beam. Normally four or five zones were irradiated looking for the signal 4 amu/e in order to measure the D_2 (main constituent) content depending on the sample position. Two points were used to measure the HD content and another two for the H_2 content. The results were averaged taking into account all the irradiated spots. This procedure was carried out for the samples wlid, wlid6, wli8, wlid10, wlid11 and wlid13. With this method the hydrogenic content is measured in all the regions of the sample. An example of the experimental details and the desorbed values obtained in the laser shots performed on the wlid6 sample is presented and Table 2. Additionally, Figure 6 shows the aspect of the sample wlid11 inside the LID chamber after applying the laser shots. In this picture, the laser spots are perfectly visible showing the removal of the lithium layer due to the pulsed laser heating. As the SIMS analyses also showed a hydrogenic content associated to the lithium layer (see section 3.2.2), the total removal of lithium would be associated to the complete desorption of the hydrogenic content. This consideration is corroborated by the profilemetry results that will be presented in section 3.2.3. They also indicated a LID crater surface with lithium absence induced by the laser heating of the Li-D film.

As the laser pulse duration was 0.25 milliseconds, the heating of the side areas placed beyond crater boundaries was probably produced. As was commented in section 2.2, the

LID procedure normally consisted in three laser pulses irradiated on each sample point. As a result of this multiple laser heating and the irregular (not perfectly Gaussian) laser profile, the non-homogeneous heating of the spot and the diffusion of a part of the hydrogenic molecules from the LID crater to their boundaries can occur. Consequently, the associated trapping of hydrogenic particles on these zones could prevent the desorption and LID detection of the related hydrogenic content. However as the vast majority (85-90%) of the hydrogenic content was desorbed during the first shot (see Figure 7), it seems logical to think that the subsequent diffusion during the additional LID shots did not produce a significant loss in the hydrogenic measurement. Additionally, the matrix effect produced by the repeated laser shots could contribute to disturb the desorption process of a part of the retained hydrogenic species. However the observation that the majority of the hydrogenic content was released during the first laser pulse seems to indicate that the contribution of this matrix effect can be also considered as non-significant. Related to this particularity, it is also important to mention that the profilemetry analyses performed on the LID craters showed a smooth surface without the irregular morphology associated to Li content (see section 3.2.3 and Figure 14) thus indicating the total removal of the Li-D content on such surface. Additionally, TDS was applied in two samples for the absolute quantification of the hydrogenic content and the corroboration of the LID results. As the section 3.2.1 shows, these TDS results obtained a maximum estimation for the deuterium retention in the order of the LID results, lower in a 30% factor. This experimental fact also indicates that the LID results did not underestimate the retention in the W-Li samples. For all these reasons, although the irregular heating, associated diffusion and matrix effects on the treated samples played a role during the measurements, it seems reasonable to think that they did not significantly affect to the desorption phenomenology and to the real retention values.

Concerning to the spatial distribution of the retention on the samples, the LID results generally showed dispersion on the desorption measurements depending on the position of the analysed spot. In general, for all the samples the lower-left, and the centre zones presented higher contents of hydrogen isotopes, probably due to the proximity of these parts to the effusive lithium cloud output of the oven and the concomitant increase in the deposition of lithium on these zones. Effusive fluxes decrease with the square of the distance from the effusion orifice, so upper parts should show a lower content of lithium

that would determine a smaller hydrogenic uptake. In addition, centre and upper centre parts also present higher contents compared to right-upper zones of the sample. The average values for deuterium and hydrogen retention are presented in Table 3 for the analysed samples depending on the Li-D_2 exposure and its surface temperature,

3.2. Post mortem analysis for W-Li-D film characterization

3.2.1. Thermal Desorption Spectroscopy

Figure 8 shows the result of the TDS analysis performed on the sample wlid11. The heating rate during the first instants of the analysis was around 11 K/s. A maximum temperature of 570ºC was reached on the sample surface. Two clear peaks are visible in the TDS spectrum, the first and bigger one at 500ºC of surface temperature and the second one (smaller) at 550ºC, being these results in agreement with previous findings in TDS experiments performed on W-Li films [14]. Assuming that water, hydrogen and other impurity contributions are negligible, the deuterium retention resulted in $1.3 \cdot 10^{18}$ cm^{-2}, value that agrees reasonably with the LID results ($2.0 \cdot 10^{18}$ cm^{-2}), being them comparable. Theoretically, the total decomposition of pure lithium hydride (mostly LiD in this case) takes place at temperatures close to 700ºC. For LiD-Li mixtures the decomposition temperature for the hydride depends on the external pressure [13]. As the maximum temperature achieved by the sample during the TDS is 570ºC, some lithium deuteride particles could remain on the surface after the TDS, thus explaining the lower deuterium retention values obtained by TDS compared to the obtained by LID. However, under high vacuum conditions (very low D pressure) the LiD molecules can be depleted at lower temperatures [12-13], showing these results total D release at similar temperature to the reached during this TDS experiment. In any case, although this TDS global value is smaller, it is necessary to take into account that deposition of lithium and the concomitant D uptake on the W-Li films were not homogeneous (see profilemetry results section, numbered as 3.2.3). Moreover, the LID technique could induce desorption from adjacent parts of the treated spot, thus including a bigger desorption area and producing an overestimation of the obtained deuterium retention. To investigate the possible presence of deuterium (mainly in the form of LiD) after the TDS, the sample wlid11 was transported again, following the protocol to avoid its contamination, to the LID chamber in order to corroborate the total hydrogenic removal on the sample by the TDS technique. Several LID shots were implemented on the outgassed surface to measure desorption of the different hydrogenic species. While no

desorption of D_2 and HD related peaks was visible, tiny H_2 related peaks, that are probably related to the unavoidable contamination with the residual vacuum during pumping period prior to the new LID measurement, were obtained resulting on values of $H_{ret}=3\cdot10^{14}$ cm^{-2}. These results imply:

- Total deuterium removal and no LiD remaining on the whole sample after TDS
- 99.9% of hydrogen removal on the sample with a maximum surface temperature of 570ºC induced by TDS
- Differences between global (TDS) and local (LID) deuterium retention values that could be explained by the limited accuracy related with the TDS measurements, the inhomogeneity of the films, the overestimation of the LID desorption area or other experimental uncertainties

3.2.2. SIMS analysis

Figure 9 presents the mass scan for light elements (0-80 amu/e) performed for the sample with highest Li/D content (wlid6). It shows the presence of hydrogenic molecules and Li isotopes in high intensity peaks that even saturate due to the high content on the sample and the high sensitivity of the SIMS detector for these species. Another big peaks present at 12-14 amu/e can correspond to the detection of Li_2 clusters formed on the beam plume. Although on this sample the lithium content was the highest and consequently, the concomitant associated impurity content is probably the larger, the presence of Li oxides resulted minority as the associated peaks (amu/e 28-30) are small. There is no presence of lithium hydroxides and carbonates peaks. It demonstrates that the conservation and transportation of the samples during all the experimental procedure was adequate, avoiding the significant contamination of the Li-D containing films. Figure 10 shows a second mass scan covering the m/q range from 180 to 220 in order to recognize the W isotopes (amu/e 182-186) and the possible associated oxides (amu/e 198-202) and lithium combinations (amu/e 188-193). In this scan four W isotopes (182, 183, 184 and 186) are visible, belonging the highest peak signal to ^{184}W. Small peaks associated to the combination of lithium isotopes with tungsten (amu/e 189-191 and 193) and tungsten oxides (amu/e 196-200 and 202) are also visible. These clusters can be produced as a result of the interaction of sputtered W and Li atoms with the oxygen ions in the beam plume.

Equivalent static SIMS analyses were performed for the samples wlid8 and wlid12. For the wlid8 the presence of lithium on the sample was clearly registered. Again, the peaks related with lithium contamination were not significant (Li oxides and hydroxides) or non-existent (lithium carbonates). It is important to note that the absolute quantification with SIMS depends on various parameters (relative sensitivity factors –RSF- of each compound) that need difficult (virtually impossible) calibrations with standards that were not available for their determination. However, the SIMS analysis showed absolute intensities of lithium that were at least a factor 20 higher (in the case of the wlid6 sample with highest Li content) compared to oxygenic Li impurities. For the case of the sample wlid8, with lower Li content, the signals of the associated impurities were even lower compared to de Li SIMS signals. Assuming RSF values not very different for lithium and their impurities, it is logical to think that the impurity content is much lower compared to lithium. The corresponding mass scan from 180-220 amu/e also showed the peaks associated to W isotopes and their oxides but not the W-Li cluster peaks. It could be related with the smaller lithium concentration on sample, experimental fact that is corroborated by the dynamic SIMS results that is shown in Figure 11.

For the blank W sample, some peaks showed the presence of lithium. However, no deposition of lithium was performed during the sample preparation. Probably this detection was produced due to previous contamination of the chamber. The level of lithium contaminated compounds (oxides, hydroxides…) was also negligible. In the second static SIMS on this sample the W peaks and their oxides dominated the spectrum while associated lithium was not detected, thus pointing to the formation of W-Li clusters in the beam plume after the sputtering of these species induced by the impinging beam. As the blank sample does not present any Li content on surface, these W-Li clusters cannot be formed and consequently they did not appear in the static SIMS spectrum.

Figure 11 presents the comparative dynamic SIMS results for the non-overlapping signals on the sample wlid6, wlid8 and the W reference sample (wlid12). In this plot the signals are normalized to the signal at 16 amu/e that corresponds to the oxygen primary ion beam used for the analysis, in order to detect differences in the ion beam fluence that could affect to the extracted results. The highest content in Li and D for the wlid6 sample is clearly visible. Comparing the both pre-lithiated samples, the intensity of the Li and D_2 signals is one order of magnitude higher in wlid6. Moreover, the temporal

evolution suggests that the Li-D thickness of the wlid6 sample is at least larger by one order of magnitude compared to the wlid8 sample as the analysis time necessary for the saturation of the involved signals is a factor 20 greater. Respect to the signal related with lithium deuteride (Li^7D at 9 amu/e) it presents a significant intensity for the wlid6 sample being this signal much bigger compared to wlid8. Consequently the presence of LiD in the W-Li film seems evident. For wlid8 the signal is at the same level as the W blank (noise level), thus suggesting the absence of lithium deuteride in this sample. The normalized profiles of D_2 and Li for samples wlid6 and wlid8 are presented in Figure 12 in order to correlate Li and D_2 depth profiles on the sample and study the chemical interaction and association of both elements. The Figure shows completely coincident profiles for Li and D_2 in both samples. It reveals deuterium retention on samples associated to the lithium layer present on the surface.

Finally although the SIMS technique does not allow an easy and direct absolute quantification of the components, as the absolute calibration of this technique is extremely challenging and requires specialized standards, the dynamic results shown in the previous figures were normalized to the W^{184} profile obtained for the wlid12 (W blank) sample. This procedure allows an approximate and relative semi-quantification of the D content by the comparison of the profiles for wlid6 and wlid8. The results of this analysis are represented in Figure 13.

The comparison of the normalized D_2 profiles for wlid6 and wlid8 reveals values of the D_2 signal normalized to W that are a factor 20-100 times higher for the case of wlid6 sample. Furthermore, the necessary time for the saturation of the D_2 related signal is larger (factor 25) for wlid6 sample. These results would indicate a dramatically lower D uptake in the case of wlid8 sample that could be roughly estimated as a difference in a factor 500-2500. The LID results indicated absolute D content (1300 lower) in wlid8 sample. Consequently, the SIMS analyses qualitatively corroborate the absolute quantification of the LID technique. Additionally, they indicate important results about the composition of the W-Li films:

- Presence of lithium deuteride in the sample wlid6 (exposed to D_2 at 200ºC), but not in the sample wlid8 (pre-lithiated and exposed to D_2 at 300ºC)
- Very low contamination of the samples with lithium oxides and hydroxides
- Association of deuterium to lithium in the studied films.

3.2.3 Profilemetry measurements

The vast majority of the LID produced craters were measured by profilemetry. Additionally, the remaining Li-D layer present of the sample surface that was not irradiated by the laser was also measured in order to study the morphology and the thickness of the Li films. It is important to note that the laser beam irradiation was able to produce craters on the Li surface of the Li containing samples, but not on the W surface of the samples where lithium was not deposited. This experimental fact was observed in the case of the blank tungsten (sample wlid12). For future experiments, however, it seems interesting try to irradiate other samples (perhaps containing CH films) in order to compare the morphology of the LID produced craters and the concomitant spots produced by our laser by using post-mortem profilemetry.

As a consequence of the experimental LID procedure, where 2-3 laser shots were applied to each sample point in order to remove all the hydrogenic content, the measured crater diameters were probably a little larger compared to the created after a single shot. It is important to remember that these analyses were carried out in atmospheric conditions. Under such conditions, the lithium films were transformed into lithium carbonate (Li_2CO_3). Lithium carbonate films are affected by swelling effects induced by its high hygroscopic activity, thus altering (increasing) the thickness and the state of the Li films. Consequently the estimation of the real (original) lithium film thickness was not possible. The Li film surface measurements showed a irregular morphology with pronounced spikes and valleys. The height of these surface spikes resulted substantially larger compared to the lithium average thickness obtained by FAES, (see section 3.2.4) due to the previously commented swelling effects. This irregular deposition originated the presence on the sample of zones with intense lithium coverage together with other with Li shortage. As these analyses were carried out after applying the alignment protocol, this irregular morphology did not result of any sample inclination and hence the measured irregular morphology surface was likely produced due to the irregular Li deposition and the swelling effects derived from the carbonate formation. Regarding the crater diameter measurements, as all the surface is assumed to be homogeneously attacked, the footprint of the LID crater size (diameter) can be considered unaltered. Moreover the interior surface of the LID crater did not present the characteristic irregular surface, with spikes and valleys, characteristic of the adjacent sample zones non-treated with LID that is associated to the Li presence, thus assuring

the total Li, and concomitant hydrogenic, removal on the LID spots during the laser irradiation. An example of the profilemetry measurements can be visualized in Figure 14. Averaging the profilemetry results for all the measured craters in the treated samples, a nominal value for the laser spot diameter was obtained:
d_{spot}=0.125±0.008 cm.

3.2.4. Quantification of lithium content on samples by FAES. Estimations of lithium film thickness.

The results of the Li thickness determination for all these samples are represented in table 4. The conversion of the FAES determinations (lithium concentration, [c_{Li}] in mg/L) to average lithium thickness originally present on sample is performed taking into account the volume (V) of the prepared lithium dissolution (50 cm^3), the area of the sample (3.6 cm^2) and the density (0.534 g/cm^3) of lithium:

$$\delta_{Li} = \frac{[c_{Li}] \cdot V}{A_{sample} \cdot \rho_{Li}} . \quad (7)$$

Additionally, it is necessary to take into account that LID (and also SIMS) is a destructive technique that implied the removal of a (small) part of the lithium layer before the FAES measurements. The measured diameter of the LID craters resulted 1.25 mm and their area 0.0123 cm^2. As and the total number of analyzed spots in each sample were normally 8, hence, the total lost area due to LID analyzes, is ≈0.098 cm^2. The SIMS spots were much smaller compared to the LIDS ones (<0.5 mm of diameter) and for all practical purposes they can be considered totally negligible. Taking into account the removed area associated with the LIDS spots and the total sample area covered by lithium (3.6 cm^2), this “lost area” and the concomitant lost mass is around 2.7% of the total. These lithium losses were added to the total amount determined by FAES.

In order to globally analyse the Li uptake obtained for the different samples, in principle, the incident lithium flux to the deposition areas from evaporative sources depends on the surrounding pressure that affects to the mean free path (λ) of Li atoms. This parameter is influenced by the collisions of the Li atoms with the gas particles present in the chamber during the evaporation and can be considered as inversely proportional to the pressure. A detailed calculation taking into account these effects can be found in [41]. However, an exhaustive analysis of the lithiation environment

dependency on the Li deposition thickness is out of the scope of this work. The second factor that influences the Li uptake by the tungsten sample is the surface temperature. Melting point of lithium is 180.5ºC. Beyond this temperature, lithium atoms will be in liquid state and the vertical configuration of the sample can induce the slipping and dripping of lithium that decreases the net uptake. Moreover, at temperatures higher than 350ºC the evaporation of lithium from the sample surface begin to affect to the deposition, as the remaining Li atoms can be evaporated in a significant fraction that will increase exponentially with the surface temperature. At lower temperatures the evaporation rate on the sample surface can be considered as negligible. Hence, beyond 350ºC on the sample a competition regime between the deposition of Li atoms from the oven and the evaporation of Li on the hot sample surface would be achieved. Comparing the results of the FAES analysis for different $T_{surface}$,at the same deposition conditions, a clear trend is visible for all the samples independently of the deposition type. The Li deposited thickness decreases at higher temperatures, being the obtained values an order of magnitude lower for temperatures of 400ºC compared to the case of 200-225ºC. At this point, the global quantification of the evaporation, dripping and slipping, for the pre-lithiated samples, effects with surface temperature and the direct comparison between different samples seems difficult to evaluate. Nonetheless, the found effect of the surface temperature in the Li film formation is clear and has great importance, as a $T_{surface}$ = 400ºC, for the Li deposition or for the subsequent D_2 exposure, determines very thin lithium films (≤100 nm) on the tungsten substrate for all the studied experimental conditions, thus precluding the potential formation of thick Li co-deposits on the W surfaces of plasma shadowed or remote zones that could be specially problematic in a fusion reactor combining liquid Li and W PFMs.

3.3. General summary of the experimental results.

The global quantitative results obtained from all the experiments and analyses are presented in table 5. After the quantitative and qualitative evaluation of the totality of them, the following experimental findings can be extracted:

- The LID technique has been developed for fuel removal and retention measurements (absolute quantification) in W-Li films exposed to molecular deuterium. A T_{rise} > 600 K for the whole sample during the LID pulse is obtained from simulations. Additionally the total Li removal in the irradiated spots was visualized with profilemetry. The SIMS measurements also

established that the hydrogenic content is associated to the Li layer, thus assuring the total elimination of such species during the laser irradiation.

- The D uptake on W (at 225ºC) exposed simultaneously to Li and D_2 in a so-called thermal co-deposition regime (simultaneous deposition of Li and D_2) is below the limit of detection of the LID technique, being the measured global D interaction for a Li film with 2 µm at the same level compared to the retention measured on the pure tungsten sample (wlid12).
- For the case of the pre-lithiation+D_2 exposure sample preparation regime the three values obtained for D_{ret} at 200ºC are very reproducible ($\approx 2.0 \cdot 10^{18}$ cm^{-2}).
- In this regime, the D retention exhibits a strong (non-linear) dependence with the surface temperature on sample. At 300ºC, the D_{ret} is reduced in a factor 1300, while at higher temperatures (400ºC) the amount of D atoms retained on the W-Li layer is decreased in a factor 50000 compared to the case of $T_{surface}$=200ºC. Hence, the Li-D interaction in liquid thin films deposited on W is substantially reduced for $T_{surface} \geq 300$ºC.
- About the hydrogen retention measurements, as the samples were not exposed directly to hydrogen, this content should be related with the presence of impurities on the Li films. This experimental fact is likely produced due to the unavoidable interaction of the lithium films with the residual vacuum, and more specifically with residual water, during the experimental procedure (oven cooling time for pre-lithiated samples and pumping time prior to LID for all samples) widely explained in subsections 2.1.2 and 2.1.3. For the case of the wlid12 sample (W blank without Li content), no measurable values were obtained for H_2 retention. This observation points to the impurity growth associated to the interaction of the residual vacuum with lithium as the main cause of this hydrogen content observed in lithium containing samples.

- The deuterium content is also related with the lithium coverage. The subsequent sample heating during the D_2 exposure produces the melting and dripping of Li in the pre-lithiated samples, thus determining the formation of a thinner lithium film. This observed Li layer reduction, however, cannot totally explain the drastic differences in terms of retention found for the pre-lithiated samples exposed to D_2 at different temperatures.

- The thickness of the liquid lithium film formed on W also depends on the experimental conditions (surrounding pressure, flow regime, presence of different gas species and surface temperature). In any case a surface temperature of 400ºC, during the Li exposure or during the subsequent D_2 exposure for the pre-lithiated samples, determines a very thin Li film on the W substrate (≤100 nm).
- The relative semi-quantification of the W-Li-D films performed with SIMS analyses corroborates the LID retention results in terms of D retention. SIMS also showed a low content of associated impurities (oxides and hydroxides) besides an absence of carbonates in the lithium films .
- TDS (T_{max}= 570ºC, 10') also allows the total removal of deuterium and hydrogen from samples, being the absolute retention results comparable to the values obtained by LID.

4. Global discussion of the obtained results. Implications for an innovative fusion reactor design based on a liquid Li divertor combined with a W first wall

4.1 Thermodynamic aspects of the thermal deuterium absorption in thin Li films deposited on W.

The characterization and analysis of the W-Li-D films performed in this study reveals a strong, non-linear effect of the increasing surface temperature on the D uptake at $T_{surface} \geq 300$ºC. The global results presented in table 5 allow analysing the role of lithium coverage and surface temperature on the global D uptake for the pre-lithiated samples later exposed to D_2. Comparing the Li uptake in the samples wlid6 and wlid8, a decrease in a factor 15 is found for the case of $T_{surface}$ = 300ºC. The additional heating necessary for the subsequent D_2 exposure after pre-lithiation leads to Li removal by dripping and slipping of the liquid layer. Additionally, the Li content on the sample wlid10 ($T_{surface}$ = 400ºC) is a bit higher compared to the sample wlid8. In principle the lithium losses due to the effects of increasing temperatures will be larger at higher temperatures, hence it seems that the quantification of the global effects of the temperature (evaporation, dripping and slipping) in the Li losses are not evident, as other experimental factors (as presence of cold parts on surface, formation of lithium aggregates due to surface tension and forces, etc) and uncertainties can have an influence. In any case it is clearly visible that even for the case of a $T_{surface}$ = 300ºC (sample wlid8) the decrease in the lithium content (factor 15) on sample is not

proportional to the reduction in the D retention (factor 1300) thus suggesting that the interaction of Li deposited atoms with thermal deuterium molecules is affected and reduced with increasing surface temperatures. This assumption is corroborated by the results obtained for the wlid10 sample ($T_{surface}$ = 400ºC). As was explained previously, the lithium uptake at this temperature is not reduced compared to the pre-lithiated sample exposed to D_2 at 300ºC (wlid8). However the D uptake is a factor 35 lower. Consequently, the changes induced by increasing the surface temperature in the Li-D surface chemistry (that determines the adsorption and/or bonding of the deuterium atoms to the Li film) seems to be the most important factor that determines the drastically lower retention values obtained at increasing temperatures.

In this way, the D uptake dependence with $T_{surface}$ by the Li films deposited on tungsten would be influenced by two factors: a lower Li deposition and a reduced D uptake by the lithium atoms present on the created liquid thin film at higher temperatures, thus resulting in a synergistic combined effect that could explain the temperature dependence of the results and the extremely lower retention values measured by LID at 400ºC. In Figure 15, an Arrhenius-type plot of the D/Li ratio is shown for the three pre-lithiated samples (wlid6, wlid8 and wlid10). Assuming that the release of deuterium from the film can be characterized by a specific activation energy, a value of E_a= 1.4 eV is obtained for the process. This value is smaller than the activation energy for lithium hydride decomposition (2.0 eV, [42]), and 7 times higher than the heat of solution deduced from the T dependence of the H solubility [43], perhaps suggesting an intrinsic dependence of the D/Li ratio on the film thickness itself. However it must be noted that this result is limited to only three experimental cases. Additional experiments (at different temperatures) would be necessary to confirm this observation.

Comparing the retention rate (D/Li atomic ratio) observed in these samples with the solubility data for deuterium in lithium bulk [44], the obtained result at 400ºC after one hour of exposure to D_2 is much lower, more than two orders of magnitude, compared to the equilibrium concentrations. In this respect, it is worth noting that the pressure of D_2 used in our experiments is far larger than the expected near the remote or plasma shadowed parts of the first wall of a reactor. Thus, for 400ºC, the equilibrium pressure, that corresponds to the onset of hydride formation, is ~10^{-2} Pa and still, even with P=133 Pa, a value of D/Li more than two orders of magnitude lower than the saturated solubility limit of ~1%, was recorded at this temperature. For the sample exposed at

200ºC the retention measured is higher that the equilibrium value, thus corroborating the formation of LiD after overpassing the saturation in the deuterium solution. Finally, the sample exposed at 300ºC presented a retention value in the order of the solubility equilibrium. According to these results, the thermodynamic behaviour of liquid lithium thin films deposited on W in terms of hydrogenic absorption seems to be different compared to the case of liquid bulk absorption thus resulting in a reduced hydrogenic uptake at temperatures higher than 300ºC.Finally, regarding to the sample prepared under a Li-D_2 simultaneous exposition regime, the obtained results at low (225ºC) wall temperature indicated a negligible D retention on the liquid Li film ($\delta_{Li} \approx 2$ µm) comparable to the case of pure W. Taking into account the previously inferred results about the temperature effect in the D retention on the W-Li pre-deposited films, it seems logical to think that at $T_{surface} \geq 400$ºC, that constitutes a scenario for the proposed DEMO operation with hot W first wall, the fuel uptake associated to thermal simultaneous Li-D_2 deposition of deuterium and lithium on W would be even more reduced.

The lessons learned from this extensive experimental work are important for the evaluation of the problematic related with potential first wall zones situated far away from the divertor or plasma shadowed, where the involved Li and fuel uptake mechanisms can be similar to that used in the preparation of the thin liquid Li-D films that have been studied. These zones can be prone to thick thermal Li deposition, whose associated fuel retention could be dangerously intense. Our results have shown that an operation at $T_{surface} = 400$ºC could drastically diminish the problem.

4.2. Considerations for the fuel retention associated to the W first wall in a reactor scenario with the proposed PFM solution

At this point it is worth to assess the implications of the present results in the hypothetic operation of a DEMO-like reactor under a liquid lithium target divertor/hot W first wall scenario. For this purpose, the more important aspects in order to evaluate and compare our experimental results, in terms of Li and D retention on W, to DEMO-like conditions are related to the real Li-D fluxes expected in a reactor scenario.

Firstly, regarding the Li impurity flux, at the considered evaporative temperature of 450ºC, the associated Li evaporative fluxes, that supposes the problematic approached in this work, will dominate this scenario [16, 23]. The experimental preparation of the samples took into account this dominant contribution for the lithium deposition as the

samples were vertically located close to the Li source (oven) that simulated the liquid Li divertor. Consequently, the comparison of the (thermal) lithium uptake found for the samples compared to the hypothetical one that can be expected in vertical zones of the first wall situated away from the divertor and/or plasma shadowed seems reasonable. As was commented in section 3.2.4, the Li uptake due to effusive fluxes strongly depends (inversely) on the surrounding pressure, as well as on the inverse-square of the distance from the Li source. The pressure levels existing in the divertor region would determine a lower Li uptake on the first wall zones situated far away from the divertor as is explained in [41]. Consequently it is quite likely that the first wall areas, that potentially suppose the object of study of this work, will not be exposed to higher pure evaporative lithium fluxes compared to the samples studied in our experiments. For the case of the Li impurity flux due to the sputtering contribution, that has not been approached in our experiments, a rigorous study showed [21] that in liquid state, approximately 65% of the Li sputtering by hydrogenic bombardment is in the form of Li^+ ions. The electromagnetic forces generated at the SOL/plasma edge and acting on the Li^+ impurities can affect the transport/migration of such ions from the plasma boundary to the PFCs surface, perhaps minimizing the deposition on W of this fraction of sputtered Li^+. In any case, a part of the Li^+ ejected atoms, the sputtered neutral Li and a fraction of evaporated lithium, ionized in the SOL/ plasma edge, will be susceptible to be transported onto the first wall, increasing in this way the associated lithium and concomitant fuel deposition. Although a thorough analysis of these erosion/redeposition phenomena is out of the scope of the paper, it is interesting to comment how they can affect to the presented results.

General impurity transport considerations [45] establish that if $\lambda_{Li^+} < \rho_{Li^+}$, (where λ_{Li^+} is the lithium ionization length and ρ_{Li^+} the Li^+ Larmor radius) the Li^+ ions will prompt re-deposited on the divertor surfaces. As first case we will estimate these values for the case of thermal (evaporated at 450ºC) Li atoms. Lithium ionization length can be estimated as:

$$\lambda_{Li^+} = v_{Li} \cdot (<\sigma v> \cdot n_e)^{-1} , \quad (8)$$

where v_{Li} is the thermal velocity of Li atoms, considered at the temperature limit of 450ºC, $<\sigma v>$ is the rate coefficient for the 1st electron impact ionization of the Li atoms (that depends on T_e), and n_e the electron density. Assuming the conservative DEMO

divertor values for n_e and T_e of $2 \cdot 10^{20}$ m^{-3} and 1.5 eV respectively, we obtain values of $<\sigma v>=1.25 \times 10^{-8}$ cm^3/s and finally $\lambda_{Li^+}=6.4 \cdot 10^{-2}$ cm. The Larmor radius can be calculated using this expression [46]:

$$\rho_{Li^+} = 102 \cdot (\mu \cdot T_i)^{1/2} \cdot (Z \cdot B)^{-1} \text{ [cm]}, \quad (9)$$

where μ is the ratio between the Li^+ ion mass and the proton mass (m_{Li^+}/m_p), Z is the charge state (+1), T_i the ion temperature (eV) and B the magnetic field in Gauss units (G). Using for T_i the value of thermal temperature of the evaporated Li atoms and B=6T (equivalent to 60000 G), we obtain $\rho_{Li^+} = 10^{-3}$ cm, a value that does not match the general prompt re-deposition criterion.

For the case of neutral Li sputtered atoms, they will be ejected from the Li surface with a minimum energy content equal to the Li binding energy [47] (1.68 eV) that would determine a conservative value for its velocity. Using this value and the same values for n_e, $<\sigma v>$ and T_e, by applying the equation (8) a value of $\lambda_{Li^+}=0.34$ cm is obtained. Considering T_i equals to the Li binding energy and B=60000 G the equation (9) gives a value of $\rho_{Li^+} = 6 \cdot 10^{-3}$ cm. With these numbers and the assumed criterion, even for the most favorable case (minimum energy for sputtered atoms and minimum value for λ_{Li^+}), values of $\lambda_{Li^+} > \rho_{Li^+}$ are obtained. These numbers indicate that for conservative DEMO divertor conditions, prompt re-deposition of these evaporated and sputtered Li impurities is not likely happening. Consequently, the possible lack of local re-deposition must be taken into account for the integration of our findings in a real reactor scenario, being a modelling/simulation approach under DEMO divertor conditions completely necessary.

Secondly, exploring the predictions about the distribution of the pressure levels inside the DEMO vacuum vessel [48, 49], the molecular D_2 pressure value used in our Li-D_2 deposition regime experiments (0.67 Pa) is comparable to the expected pressures in zones close to the separatrix and SOL region. However, in the sub-divertor areas around this region, the neutral pressure decreases strongly with pressures around 0.01 Pa [48]. In the W first wall areas situated at a larger distance from the divertor region or plasma shadowed, the neutral pressure is expected to be even lower, ultimately given by the recycling properties of the material. On them, the obtained results seem representative and could be, in principle, taken into account as reasonable Li and D retention estimations. However, it is important to note that in the global first wall, the associated

larger charge-exchange (CX) and sputtering neutral fluxes may dominate the co-deposition instead the pressure.

For the global reactor first wall environment, the thermal Li and D_2 deposition scenario is not the most realistic scenario, as during the D-T reactor operation the W first wall surface would be affected by simultaneous Li and D (neutral, molecular and ionic) incident fluxes, as well as by an intense bombardment with energetic neutrons and helium ions. The influence of fuel ionic bombardment in the retention on hybrid W-Li films is expected to be quite important as the magnitude of the ionic flux, especially on first wall zones close to the divertor, will be very considerable. This ionic bombardment will produce the implantation of Li and fuel species that will affect to the tritium inventory. About this issue, it should be pointed out that previous experiments with cold ($T_{surface} \approx 100$ºC) W samples exposed to Li-seeded H_2 Glow Discharge (GD) plasmas [14] found a lower hydrogen retention compared to pre-lithiated W samples later exposed to H_2 GD plasmas, suggesting that no extra hydrogenic retention will be produced by the lithium implantation in comparison to the expected on lithium simply deposited. Additionally, very promising results have been obtained in terms of fuel retention and Li film formation for hot W samples exposed to Li-seeded deuterium linear plasmas in the PISCES-A divertor simulator [50]. These results presented in the worst case a retention (atomic ratio) at $T_{surface}$ = 400ºC higher by two orders of magnitude compared with the retention found for our sample wlid10 prepared at the same surface temperature. Despite these encouraging results, in order to have a global vision of the W-Li mixing processes, and its associated fuel retention problems expected in a reactor with the proposed PFM scenario, the fuel retention on the reactor first wall areas affected by Li deposition/implantation together with intense plasma, neutron and CX bombardment during longer time scales must be wider studied.

5. Conclusions

The presented results show a non-linear effect of the surface temperature in the deuterium retention found on thin liquid Li films pre-deposited on hot W, being this result probably related with a different pattern for the thermodynamic interaction of the thin liquid Li films with deuterium compared to the traditional case of liquid bulk absorption. Additionally, even at $T_{surface}$=225ºC, the W sample exposed to simultaneous thermal deposition of Li and D_2 showed the formation of a lithium film ≈ 2 µm thick

while the associated deuterium retention was below the sensibility of the LID technique, showing a similar behaviour compared to pure W.

Although other aspects related with the presence of high ionic/recombination fuel, neutron fluxes and the associated harmful effects in the fuel retention have not been approached, these results represent a first approximation to the problematic of the potential formation of thick Li-D co-deposits on especially problematic in-vessel reactor areas (remote from plasma and/or plasma shadowed) that could accumulate uncontrolled amounts of tritium.

The exhaustive experimental work points to that the operation with a hot W first wall (T=400ºC) would be associated to the formation of thin liquid Li films (thickness of few microns) whose associated fuel retention (in the case of only thermal molecular species) would result extremely low, at the same level compared to the retention in pure W elements (atomic D/Li ratio <0.1 at.%). This attractive result supposes an encouraging perspective in terms of retention and precluding of hydride formation on the W-Li films situated on remote or plasma shadowed areas of the W first wall that could threaten the operation of a reactor combining both PFMs due to the associated risks related with the allowed tritium administrative limits. However, it is important to note that even in future reactors, the use of a hot W first wall T≥400ºC might be not assured due to economical or engineering limitations. Additionally, several diagnostics and/or heating systems could need lower working temperatures.

For the extrapolation of these findings to the global tritium retention problematic of a DEMO-like reactor, the promising experimental results must be confirmed in experimental conditions that would include ionic/neutral and molecular Li/D fluxes to determine if this low D saturation regime found in the W-Li films can be achieved in a reactor-like regime. The possibility of exposing tungsten to Li-D_2 co-deposition environments in the recently upgraded Magnum-PSI linear device, that will enable a material exposure under experimental conditions characterized by extremely large plasma fluences and longer term exposures closer to a reactor scenario, appears very attractive for this purpose.

Acknowledgements

This research was partially financed by the Spanish “Ministry of Economy and Competitiveness” under project FIS2010-20911. A.de Castro wants to acknowledge

financial support from the PhD grant awarded by CIEMAT (BOE resolution n◦175, 23/7/2012). The authors also want to recognize to the doctors E. Oyarzabal and A.B. Martin-Rojo their valuable help in relation with the experimental work (sample transportation and manipulators installation) here presented as well as to Dr. J. González and Dr. D. Tafalla for their indications during the Nd:YAG laser tuning, Dr. F.J. Sánchez for the useful suggestions during the operation of the SIMS experimental unit and the CIEMAT chemistry department that carried out the FAES analyses. This work has been carried out within the framework of the EUROfusion Consortium and has received funding from the Euratom research and training programme 2014-2018 under grant agreement n◦633053. The views and opinions expressed herein do not necessarily reflect those of the European Commission.

References

[1] V. Philipps, J. Roth, A. Loarte, Plasma Phys. Control. Fusion 45 (2003) A17–A30

[2] R.P. Wenninger, M. Bernert, T. Eich, et al., Nucl. Fusion 54 (2014) 114003

[3] A. Loarte et al. Nucl. Fusion 47 (2007) S203-S263

[4] R. Maingi et al. Phys. Rev. Lett. 103 (2009) 075001

[5] F.L. Tabarés et al. Nucl. Fusion 57 (2017) 016029

[6] G. Mazzitelli et al. J. Nucl. Mater. 463 (2015) 1152–1155

[7] M. Turnyanskiy et al. Fusion Eng. Des. 96–97 (2015) 361–364

[8] G. Federici et al. J. Nucl. Mater. 14 (1999) 266–269

[9] S. V. Mirnov et al. Plasma Phys. Control. Fusion 48 (2006) 821

[10] M. Ono et al. Nucl. Fusion 53 (2013) 113030

[11] M. Ono et al. Fus. Eng. Des. 89 (2014) 2838–2844

[12] A.B. Martin-Rojo, et al., Fusion Eng. Des. 89 (2014) 2915.

[13] E. Oyarzabal, A.B. Martin-Rojo, et al. J. Nucl. Mater. 463 (2015) 1173–1176.

[14] A. de Castro et al. Fus. Eng. Des. 117 (2017) 212-216

[15] S.V. Mirnov et al. Nucl. Fusion 51 (2011) 073044

[16] R.E. Nygren and F.L. Tabarés, Nucl. Mater. Energy 9 (2016) 6–21

[17] J. Engbaek et al. Surf. Sci. 600 (2006) 1468-1474

[18] A.M. Capece et al. J. Nucl. Mater. 463 (2015) 1177-1180

[19] J.P. Allain, "Kinematic and Thermodynamic effects on liquid lithium sputtering" PhD. thesis, University of Illinois, May 2000

[20] M. A. Jaworski et al. J. Nucl. Mater. 415 (2011) S985-S988

[21] J.P. Allain et al. J. Nucl. Mater. 290-293 (2001) 180-184

[22] J.P. Allain et al. J. Nucl. Mater. 313-316 (2003) 641-645

[23] R. Bastasz and W. Eckstein, J. Nucl. Mater. 290-293, (2001) 19-24

[24] B.I. Khripunov et al. J. Nucl. Mater. 290-293 (2001) 201-205

[25] G. Pelka et al. Contrib. Plasma Phys. 56 (2016) 6-8, 802–807

[26] M. Poradzinski et al., EUROfusion Liquid Metal Strategy Meeting (2017), Prague, Czech Republic

[27] S. Krat el al. Vacuum 105 (2014) 111-114

[28] Yu. M. Gasparyan et al. Fus. Eng. Des. 117 (2017) 163-167

[29] A. S. Popkov et al. Phys. Procedia 71 (2015) 88 – 92

[30] C.H. Skinner et al. J. Nucl. Mater. 438 (2013) S647-650

[31] J.L. Gland, B.A. Sexton, G.E. Mitchell, Surf. Sci. 115 (1982) 623–632

[32] P. Krstic et al., Phys. Rev. Lett. 110 (2013) 105001

[33] V. Phillips et al. Nucl. Fusion 53 (2013) 093002

[34] LPY600 LITRON Laser Series Operators Handbook, 20055

[35] https://refractiveindex.info

[36] E. Siegel, Phys. Chem. Liq. 5 (1976) Iss. 1

[37] https://www.webelements.com

[38] D.W. Jeppson et al. Lithium literature review: Lithium's properties and interactions (1978), Handford Engineering Development Laboratory

[39] D.Sands, Pulsed Laser Heating and Melting, Heat Transfer - Engineering Applications, (2011) Prof.Vyacheslav Vikhrenko (Ed.), ISBN: 978-953-307-361-3

[40] H.S. Carslaw and J.C. Jaeger, Conduction of Heat in Solids, (1959) 2nd ed. (Oxford V. P., London).

[41] C.H. Skinner et al. J. Nucl. Mater. 390–391 (2009) 1005–1008

[42] E. Veleckis. J. Nucl. Mater. 79 (1979) 20

[43] H. Katsuta et al. Nucl. Technol. 32 (1977) 297

[44] P. Hubberstey et al. Journal of the Less-Common Metals, 49 (1976) 253-269

[45] Y. Homma et al. Nucl. Mater. Energy 12 (2017) 323-328

[46] J.D. Huba, NRL Plasma Formulary, (2013) Naval Research Laboratory, Washington DC 20375

[47] J. Lázsló and W. Eckstein, J. Nucl. Mater. 184 (1991) 22-29

[48] Chr. Day et al. Fus. Eng. Des. 89 (2014) 1505-1509

[49] C. Gleason-González et al. Fus. Eng. Des. 89 (2014) 1042–1047

[50] F.L. Tabarés et al. Plasma Phys. Control. Fusion 59 (2017) 044006

Table captions:

Table 1. Physical and optical properties for W, Li and average values

Table 2. LID analyzes on wlid6 sample

Table 3. Hydrogenic retention results for the samples analyzed with LID

Table 4. Numeric values (in µm) for the Li film thickness deposited on samples

Table 5. Global summary of the D, H (obtained by LID measurements) and Li (FAES determination) contents for the studied samples

Table 1.

Element	c_p, J/Kg K	ρ, Kg/m^3	k, W/m·K	D, m^2/s	Reflectance
Tungsten (W)	130	19250	170	6.79E-05	0.602
Lithium (Li)	3750	535	85	4.24E-05	0.941
W-Li (av. value)	1940	9918	128	5.51E-05	0.772

Table 2.

LID point	Analyzed molecule	Spot position	Desorbed molecules
1	D_2 (4 amu/e)	Left lower corner	1.70E+16
2	D_2 (4 amu/e)	Right lower corner	9.82E+15
3	D_2 (4 amu/e)	Right upper corner	6.33E+15
4	D_2 (4 amu/e)	Upper center	1.18E+16
5	D_2 (4 amu/e)	Center	9,76E+15
6	HD (3 amu/e)	Left center	2.12E+15
7	HD (3 amu/e)	Lower center	1.58E+15
8	H_2 (2 amu/e)	Right center	4.98E+14
9	H_2 (2 amu/e)	Left upper corner	6.96E+14

Table 3.

Sample	**D_2-Li exposure**	**$T_{surface}$, °C**	**H_{ret}, cm^{-2}**	**D_{ret}, cm^{-2}**
wlid	D_2-Li co-deposition	225	**$2.6\pm0.6\cdot10^{16}$**	-
wlid6	pre-Li+D_2	200	**$2.4\pm0.8\cdot10^{17}$**	**$1.9\pm0.7\cdot10^{18}$**
wlid8	pre-Li+D_2	300	**$4.4\pm0.9\cdot10^{15}$**	**$1.5\pm0.3\cdot10^{15}$**
wlid10	pre-Li+D_2	400	**$1.3\pm0.4\cdot10^{15}$**	**$4.3\pm0.4\cdot10^{13}$**
wlid11	pre-Li+D_2	200	**$5.9\pm1.4\cdot10^{17}$**	**$2.0\pm0.3\cdot10^{18}$**
wlid13	pre-Li+D_2	200	**$2.8\pm0.5\cdot10^{17}$**	**$2.0\pm0.6\cdot10^{18}$**
wlid12	no Li-W blank	200	-	-

Table 4.

$T_{surface}$, ºC	Vacuum conditions (no D_2)	Vacuum conditions (+ D_2)	He atmosphere	D_2 atmosphere
200	0.94	0.91* (wlid6)	-	-
225	-	-	0.45	2.00 (wlid)
300	0.47	0.06* (wlid8)	0.03	-
400	0.06	0.11* (wlid10)	0.03	-
500	-	-	0.04	-

*Samples pre-lithiated in vacuum at 200ºC and later exposed to D_2 at the temperature referred in table

Table 5.

Sample	$T_{surface}$, ºC (Li-D_2 exposure)	Li film g/m^2 (µm)	D_{ret} cm^{-2}	D_{ret} mg/m^2	H_{ret}*** cm^{-2}	H_{ret} mg/m^2	D/Li ($A_{D:Li}$)	H/Li ($A_{H:Li}$)
wlid	225 (co-deposition)	1.03 (2.00)	**	-	$2.6\cdot10^{16}$	0.43	-	0.003
wlid6	200 (pre-Li+D_2)	0.47 (0.91)	$1.9\cdot10^{18}$	63	$2.4\cdot10^{17}$	4.0	0.45	0.060
wlid8	300 (pre-Li+D_2)	0.033 (0.06)	$1.5\cdot10^{15}$	0.050	$4.4\cdot10^{15}$	0.073	0.005	0.016
wlid10	400 (pre-Li+D_2)	0.059 (0.11)	$4.3\cdot10^{13}$	0.0014	$1.3\cdot10^{15}$	0.022	$8\cdot10^{-5}$	$2.5\cdot10^{-4}$
wlid11	200 (pre-Li+D_2)	0.030* (0.06)	$2.0\cdot10^{18}$	66	$5.9\cdot10^{17}$	9.8	-	-
wlid13	200 (pre-Li+D_2)	-	$2.0\cdot10^{18}$	66	$2.8\cdot10^{17}$	4.6	-	-
wlid12	200 (no Li,W blank)	-	**	-	**	-	-	-

* Value that does not correspond to the original Li film content. Remaining Li after TDS
** Below limit of detection of the LID technique
***Hydrogen uptake associated to impurities present on the Li layer. Samples were not exposed to H_2

Figure captions:

Figure 1. Deposition chamber sketch: a) Top view, b) Front view

1. Optical windows, 2. Lithium oven, 3. Gate valve for sample manipulator, 4. Sample manipulator, 5. Ionization gauge, 6. Gas inlets (Deuterium and Argon), 7. Capacitance manometer, 8. Feedthrough for Li oven and thermocouple, 9. Gate valve for turbopump, 10. Pumping unit, 11. Sample heating element (manipulator and filament), 12. Pyrometer, 13. Tungsten sample

Figure 2. Position of the sample respect the Li effusion orifice. Angular characteristics

Figure 3. Top view of the LID chamber and Nd:YAG laser:

1. Optical windows, 2. Pumping unit, 3. Ionization gauge, 4. Residual gas analyzer, 5. Gate valves for main chamber and sample manipulator, 6. Sample manipulator, 7. Prepared sample 8. Nd:YAG laser, 9. LID vacuum chamber main body. 10. Focusing (converging) lens, 11. Primary (non-focused laser beam)*, 12. Focused laser beam*

*As the laser operates in the first harmonic (1064 nm), its beam is really invisible

Figure 4. Comparison between RGA and pressure signals during LID pulse that shows the consistency of the desorption measurements

Figure 5. LID crater present on wlid6 sample

Figure 6. Picture of the sample wlid11 situated inside the LID chamber. The spots present on the sample surface (produced by the LID shots) show the complete removal of the Li-D layer

Figure 7. Example of LIDS analysis for D_2 retention determination. The largest RGA peak is associated to the first LID shot and represents the 85-90% of the total D_2 desorption while the smallest (last) one is related with residual desorption from parts adjacent to the LID crater

Figure 8. TDS spectrum for the wlid11 sample

Figure 9 Static SIMS on wlid6 sample: mass scan from 0 to 80 amu/e

Figure 10. Static SIMS on wlid6 sample: mass scan from 180 to 200 amu/e

Figure 11. Comparative dynamic SIMS analyzes on wlid6, wlid8 and wlid12

Figure 12. Normalized Li and D_2 profiles on wlid6 and wlid8 samples

Figure 13. Li and D_2 profiles normalized to W^{184} profile (blank sample)

Figure 14. Profilemetry measurement performed on a LID crater (sample wlid6). After the laser irradiation the crater presented a smooth surface in comparison to the irregular

Li containing surface situated beyond the crater boundaries. The appearance of the crater is attributed to the complete removal of the Li-D layer produced by the LID pulse

Figure 15. Arrhenius plot for the D/Li ratio obtained for samples wlid6, wlid8 and wlid10

Figure 1.

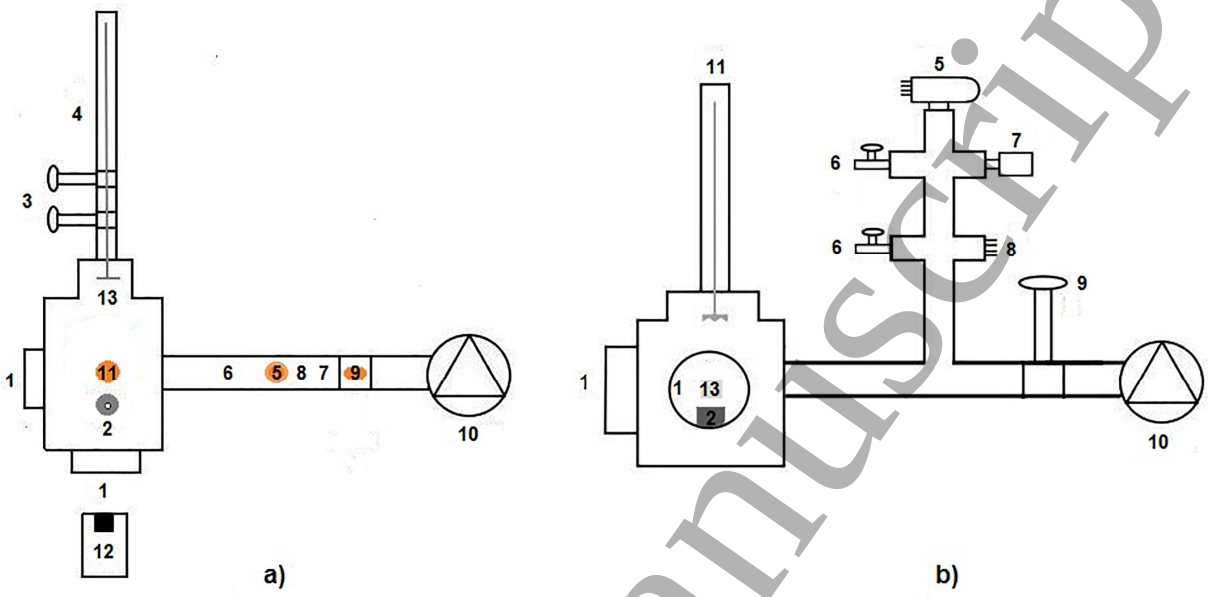

Figure 2.

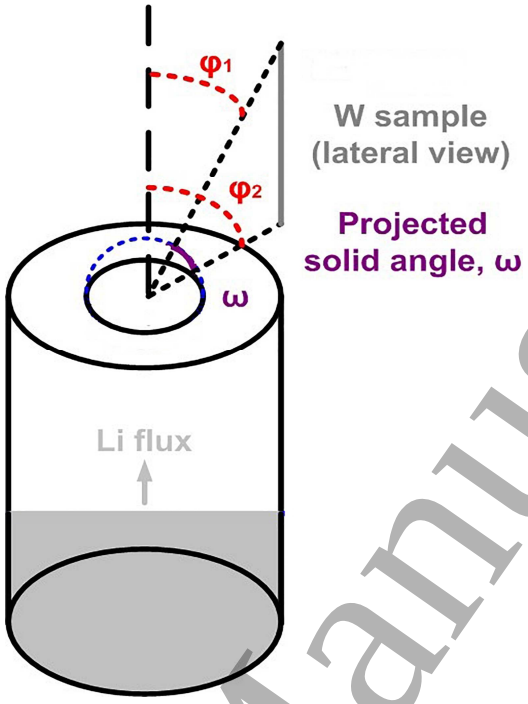

Figure 3.

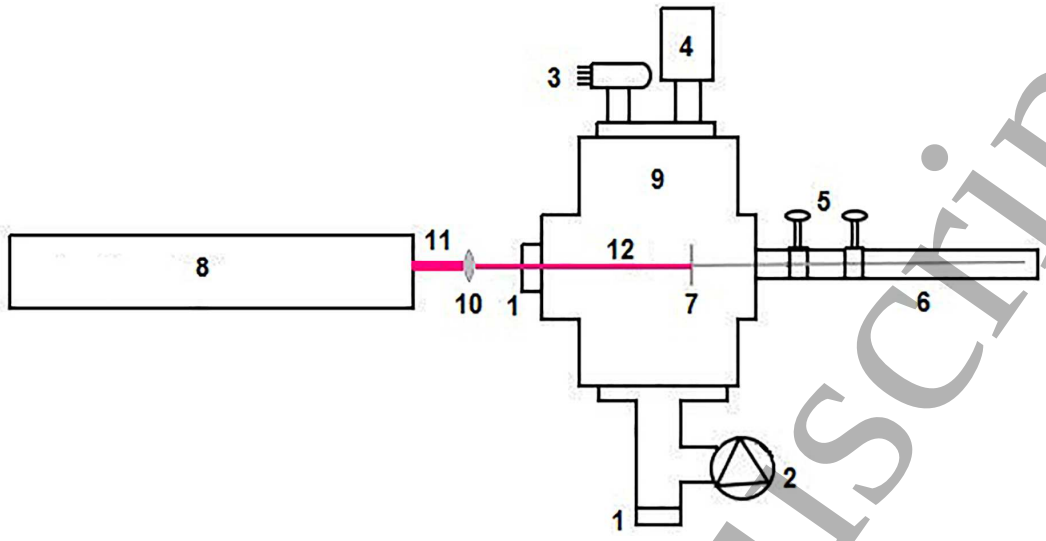

Figure 4.

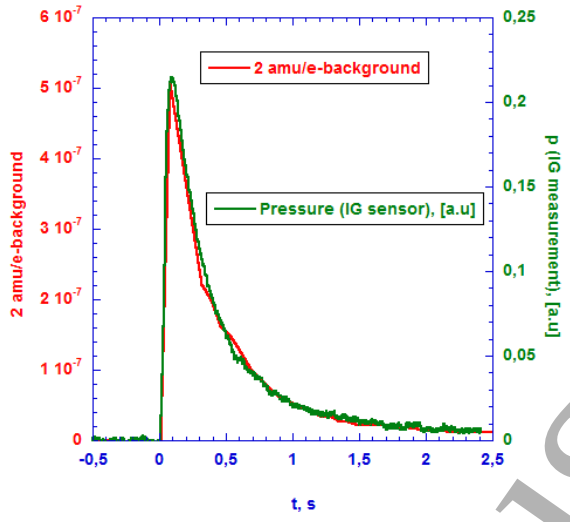

Figure 5.

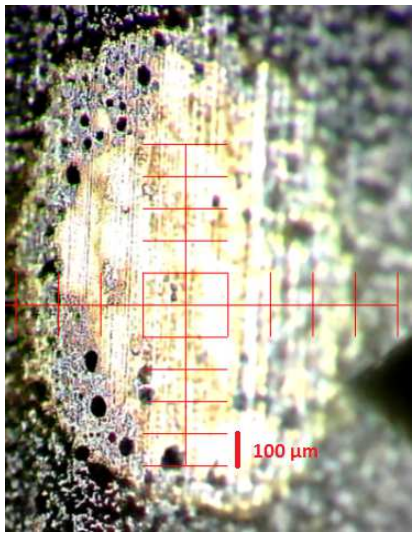

Figure 6.

Figure 7

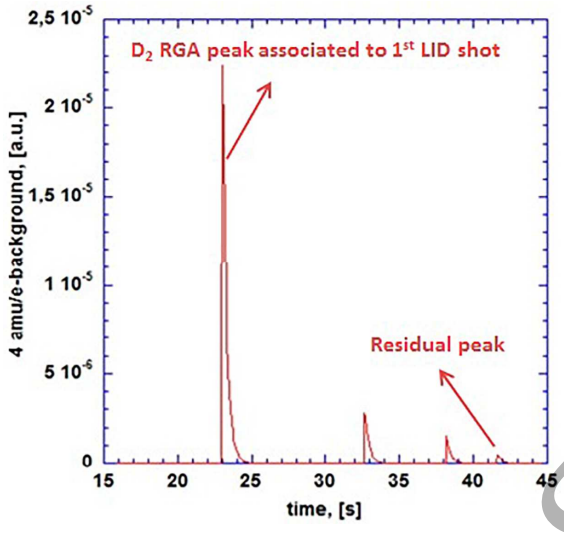

Figure 8.

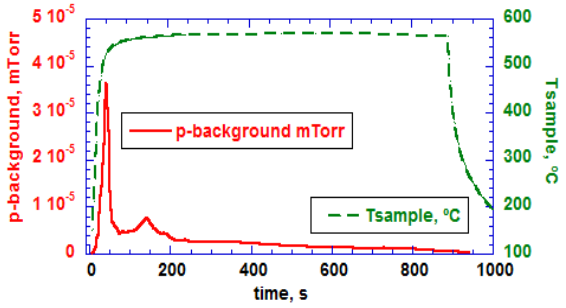

Figure 9.

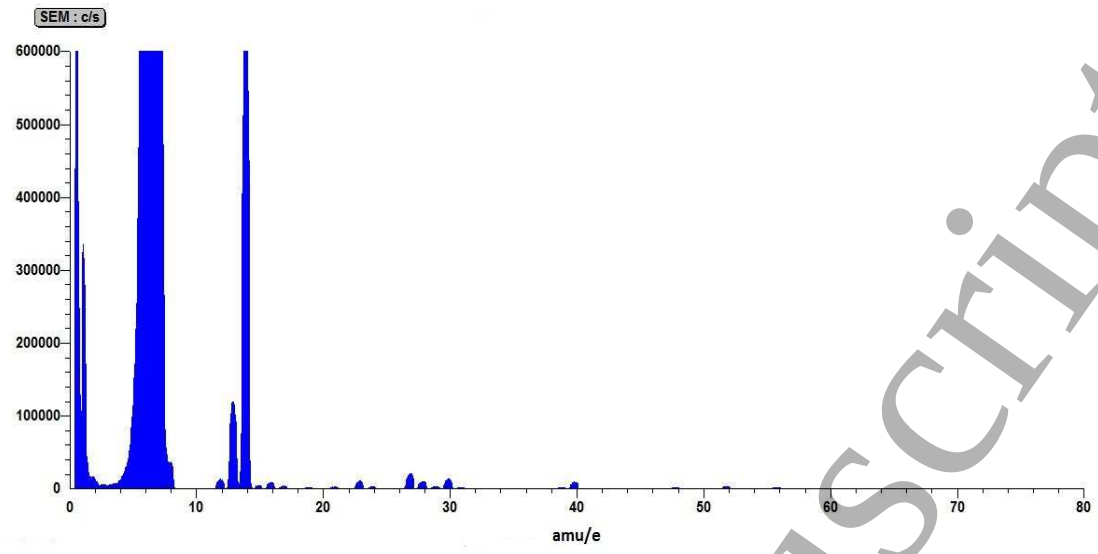

Figure 10.

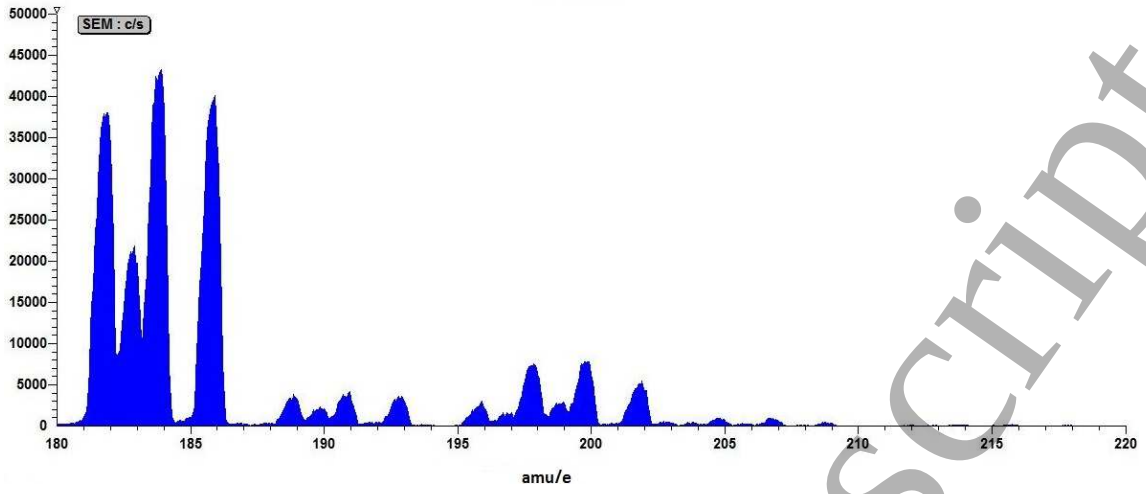

Figure 11.

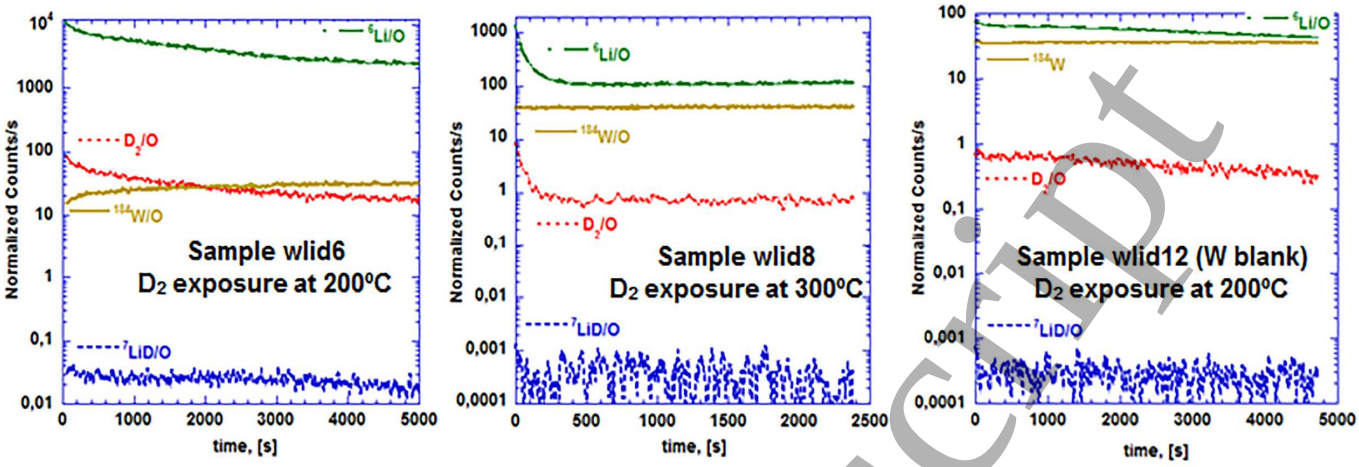

Figure 12.

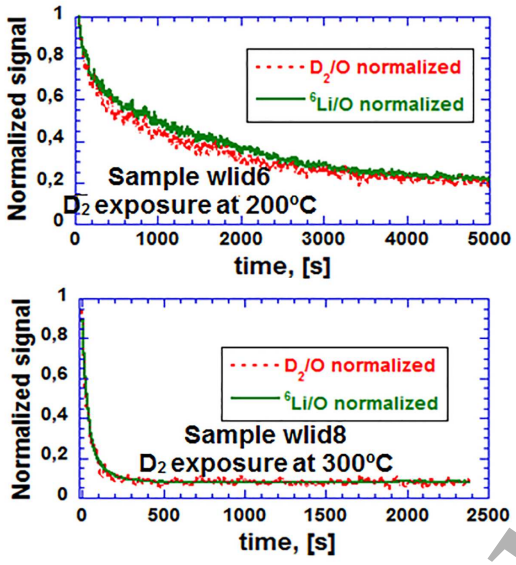

Figure 13.

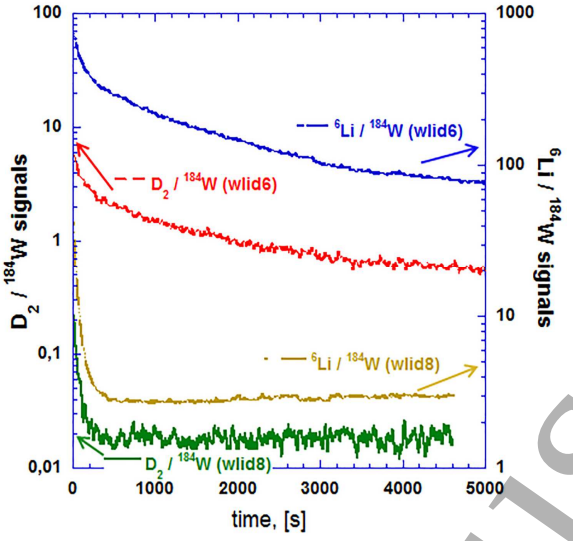

Figure 14.

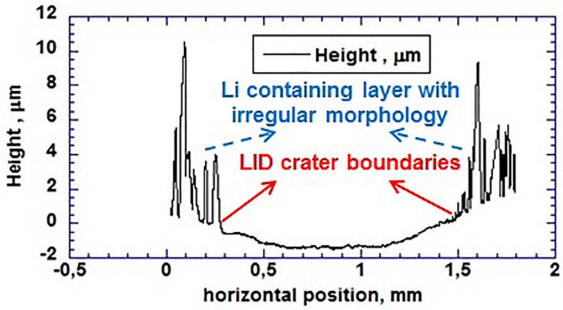

Figure 15.